Check for updates

Received: 27 October 2020 | Revised: 5 January 2021 | Accepted: 18 February 2021

DOI: 10.1002/amp2.10081

RESEARCH ARTICLE

JOURNAL OF ADVANCED MANUFACTURING AND PROCESSING WILEY

Tri-fold process integration leveraging high- and low-temperature plasmas: From biomass to fertilizers with local energy and for local use

Mohammad M. Sarafraz[1,2] | **Nam N. Tran**[2,3] | **Hung Nguyen**[1,4] | **Laurent Fulcheri**[5] | **Rachel Burton**[6] | **Peter Wadewitz**[7] | **Gregory Butler**[8] | **Lawrence Kirton**[9] | **Volker Hessel**[1,2]

[1]School of Engineering, Warwick University, Coventry, UK

[2]School of Chemical Engineering and Advanced Materials, University of Adelaide, Adelaide, Australia

[3]Department of Chemical Engineering, Can Tho University, Can Tho, Vietnam

[4]Teletraffic Research Center, University of Adelaide, Adelaide, Australia

[5]MINES ParisTech, PSL-Research University, PERSEE, Sophia-Antipolis, France

[6]Department of Plant Science, School of Agriculture, Food, and Wine, University of Adelaide, Adelaide, Australia

[7]Peats Soil and Garden Supplies, Whites Valley, Australia

[8]South Australian No-Till Farmers Association, Clare, Australia

[9]AgGrow Energy Resources Company, Perth, Australia

Correspondence
Volker Hessel, School of Chemical Engineering and Advanced Materials, University of Adelaide, Adelaide, Australia.
Email: volker.hessel@adelaide.edu.au

Funding information
European Commission, Grant/Award Number: 810182; University of Adelaide, Grant/Award Number: Pro-Vice Chancellor Travel Grant - Laurent Fulcher

Abstract

In the present study, a series of thermochemical equilibrium modeling was conducted to assess the thermodynamic potential of biomass conversion to ammonia using thermal and nonthermal plasma at small- and large-scale production. The system was designed and evaluated for five different locations in Australia including the Northern Territory, South Australia, Western Australia, and New South Wales using local biomass feedstock. The equilibrium modeling showed that the pathway of biomass to biomethane using an anaerobic digestion reactor, biomethane to hydrogen using a thermal plasma reactor, followed by conversion of hydrogen to ammonia via a nonthermal plasma reactor is a plausible route, by which the exergy efficiency of the process can be as high as ~60%. It is identified that the thermal plasma reactor required two distinct zones at $3000^{\circ}C < T < 4000^{\circ}C$ and $1500^{\circ}C < T < 2500^{\circ}C$. The first zone aims at converting electric energy into very high temperature thermal flow while the second one enables to split methane molecules into solid carbon and hydrogen. The new ammonia process is also assessed from the viewpoint of the current industrial transformation, being accelerated by the post-COVID economy, which moves toward local, resilient, integrated and self-sufficient production under the umbrella of an emerging fractal economy. With respect to local production, the developed process is designed for a quick response to farm use and on-time production in view of the demands of modern ICT-sensor based precision agriculture. The proposed process was found to be flexible ("resilient") against production scale, geographical location, price and type of feedstock, and source of renewable energy. The system was found to be flexible against different feedstock such as spent grape marc, mustard seed, bagasse, piggery and poultry. The system can be self-sustained up to ~80% at $T = 3500^{\circ}C$; with the thermal plasma reactor-zone 2 producing the electricity requirements for the nonthermal plasma

This is an open access article under the terms of the Creative Commons Attribution-NonCommercial-NoDerivs License, which permits use and distribution in any medium, provided the original work is properly cited, the use is non-commercial and no modifications or adaptations are made.
© 2021 The Authors. *Journal of Advanced Manufacturing and Processing* published by Wiley Periodicals LLC on behalf of American Institute of Chemical Engineers.

via a steam turbine power block. Finally, the system it is investigated to which degree the system is adaptable to local production, self-sufficient, and circulatory.

KEYWORDS

ammonia production, biomass anaerobic digestion, circular economy, nonthermal plasma, process integration, renewable energy, thermal plasma

1 | INTRODUCTION

1.1 | Global mega-scale or local production? A post-COVID re-visit

In the last two centuries, the industrial revolution has delivered ever-larger production capacities as an economically viable concept.[1] From those mega-manufacturing sites, the products are to be distributed by comparatively inexpensive transport all over the world, increasing welfare. Chemical production has taken this concept of large scale, and chemical plants went well above the scale of a million tonnes per year.[2,3] Moore's Law has become the directive for economic growth.[4]

Yet, this globally successful model is not in each case optimal for national economies and in the recent time a refocusing on local production is observed as anti-trend; to prevail independence of global market dependencies. The COVID pandemic has amplified those threats of the effect of negative supply and demand shocks on the aggregate output.[5] COVID has led to a reduction of the global production of the chemical industry by 1.2%, which is the worst decline for the sector since the 2008 financial crash.[6] Major chemical manufacturing companies such as BASF exerted a slowdown in predicted growth.[7] Those complementarities in consumption and production amplify each other.[8]

Thus, the current economic environment asks for an antithesis to the economy of scale[4] in its shape of a neoclassical model.[8] This strategy is centered on the sensitivity to place and scale to sustain local communities and to provide new job opportunities while preserving the quality of the environment. This punctuates the move from a traditional centralized, large-scale, long lead-time forecast-driven production operation to the new paradigm of decentralized, autonomous manufacturing near end user-driven activity.

1.2 | Self-sufficient decentral production

The COVID crisis caused recentering on local production has proposed the self-sufficient local economy, which marks the decentralization of all economic activities and is based on small or medium-sized production facilities within the same revenue district.[9] The production of this revenue is to a large share consumed in the same district, that is, at the spot. All economic activities take place within the revenue district itself, and only raw material not available has to be imported from elsewhere. Such a self-sufficient revenue district is termed a fractal economy or a nonlinear production model.[8] The extending provincial economy is composed of a large number of such fractal economies. The extending national economy will comprise of a set of provincial fractals. Taleb terms such as functional units as Fractal Localism.[10] The Fractal Economy is believed to be anti-fragile,[11] tolerating not stress and pressure, and thereby supports thriving and growing. A key to drive up cost-competitiveness capacity and efficiency constraints sit in the domestic transport infrastructure, and possibly minimization of that is the right principle. There is a strong opportunity to boost global cost competitiveness with cheaper domestic pricing and availability. Historical experience suggests that unlocking supply is critical for supporting future demand growth.[12]

Sustainable sourcing and local manufacturing support the concept of *Slow Fashion*, which is a philosophy of attention that is sensitive to environmental and societal needs and the impact of production and distribution on society and the environment.[13] Local manufacturing also promotes the concept of *Corporate Sustainability*, which is a business approach to create long-term shareholder value by managing risks of economic, environmental and social developments. Finally, the new approach is assorted to *Massification*, which is a business model encompassing fast cycles, rapid prototyping and small product batches with larger varieties.

The concept of local manufacturing leads to fast techno-economic cycling in today's Australia, showing the industrial transformation from fossil to renewable fuels and from environmentally unfriendly resource extraction to more benign technologies. This asks for a supplement of Australia's strong primary industries (energy, mining, food) by an upheaval of secondary industries (fertilizers, biomass, and horticulture).[14–17]

Those innovations will only flourish in the suction of the primary industries, and thus heavily demand process integration. In chemical terminology, that relates to the BASF-invented Verbund strategy, which has been taken over by the global chemical industry.[18] Such an approach could inter-relate Australia's agriculture and energy markets.

1.3 | Future factories: An enabler for local manufacturing

Europe has started a decade ago with the vision of Future Factories, providing opportunities, which the conventional plants do not meet.[19] Europe's "chemical plants of tomorrow" are envisioned as compact container plants to speed up process development and offer as well as advantages for chemical production.[20] Those plants are mobile (Evonik's "Plants on Wheels[21]" and the "50% Idea[22]" of the German chemical industry and academia) and can utilize renewable energy (Evonik's "Fertilizing with the Wind[23]"). That opens the door to entirely new business models for distributed production at the local site of farming.

1.4 | Fertilizer local production

Against this backdrop, Evonik Industries have targeted the local manufacturing of fertilizers by low-temperature plasma technology as a key for precision agriculture.[24] Fertilizers and ammonia as their key chemical are essential to global welfare.[25] Ammonia ranks second, to sulfuric acid, as the chemical with the largest tonnage; in 2016, 146 million tonnes of ammonia were produced.[26] While techniques for the production and purification of ammonia have been further investigated,[27–29] locally produced fertilizers cannot compete with industrial manufacture on a giant scale such as 1 million tonnes per annum or more. Yet, those fertilizers can be supplied just below the economic bar, and our previous calculations have forecasted a higher price by a factor of 3 to 6.[30] Those disadvantages in scale (1–10 kt/a vs. 1 Mt/a) can be partially compensated by beneficial fixed costs, given by pre-manufacturing of modules, earlier break-even (higher net-present value), and lower interest rates due to confirmed performance.[31] Yet, the real economic benefit of the localized plasma production plants is to be a resilient enabler to overcome regional economic disadvantages, such as in Africa, high taxes and high transport costs,[30] their integration into a new self-sufficient economy (see above), and to thrive the regions toward local autonomy and foster local job creation.

1.5 | National drivers of local fertilizer economy: The Australian situation

To better understand this disruptive opportunity, it is worth to make conscious of the Australian farming situation. Rainy and very dry periods take turns.[32] Fertilizer consumption is high in rainy sessions and low in dry ones. There is no real precision Agtech answer today to this challenge—farmers store an average amount of fertilizers in their storage tanks as a pragmatic comprise. Similarly, the acidification of soils is hardly addressed, which globally adds costs for environmental damage of about $1.6 billion/year.[33] In Australia, the salination of soils also causes costs of $187 million/year.[34]

1.6 | Integrated fertilizer manufacture process design: Biomass/thermal plasma/nonthermal plasma

It is our perception that even the most advanced biomass technologies are a tough act to follow, as compared to the cheap oil economy.[35,36] The way out of this dilemma is the integration in a different economic pathway that might offer a solution to reach an economic scale. On the other end of the commercial food chain, low-temperature plasma processes have shown promise for the nitrogen fixation to fertilizers.[24,37–40] While they seem to be on the way to give an economic pathway to nitric acid as platform material for fertilizers recent plasma technologies did not manage to produce truly green and affordable ammonia.[41–43] Having both ammonia and nitric acid would open the full N-based fertilizer plethora from urea, ammonium nitrate, potassium nitrate, and so on.

The missing leap is a green conversion of biogas, (biomethane) after enrichment from its dilute constitution in biogas, toward blue or green hydrogen. Hydrogen accounts for about 70–80% of the sustainability footprint of ammonia. The thermal plasma splitting of methane into green hydrogen and solid carbon is such technology.[44–4544,46] It is about seven times more energy-efficient than water hydrolysis, to which so much promise is currently given as green hydrogen technology.[44] It co-valorises solid carbon, and it is beyond the scope of this manuscript to outline that economic benefit; yet likely it is substantial.

The thermal plasma methane pyrolysis process to blue hydrogen has recently been transferred from pilot to industrial scale. A first industrial commercial plant of 14 000 and 4600 tonnes per year capacity for solid carbon and hydrogen, respectively, has been erected by MONOLITH Materials, inc. in US-Nebraska.[44,46]

1.7 | Industrial directives as boundary conditions of this study

The process design study considers commercial constraints and opportunities as its boundary conditions. Data are taken from a commercial product and business opportunity of Peats Soil Company that look for fertilizer manufacture at the point of manufacture at an industrial site. They are interested in upgrading their smart compost pellet product (composition: 12% total C; 1% N; 0.2% P and 0.5% K) to 20% higher carbon and 3% higher nitrogen content by locally manufactured carbon (activated carbon, biochar) and ammonia. They like to prevent fertilizer leaching by complexation to carbon carriers. The commercial fertilizer opportunity on a national farmers' scale has been defined by the South Australian No-Till Farmer Association (SANTFA); with a view on the personalization of fertilizer products, its customization for individual users, and an outlook to its user-friendly enhanced and environmentally benign product functionality. SANTFA provided foresight on the impact of fertilizer choice and complexation to carbon carriers on soil acidification and effective usage (leaching prevention). AgGrow Energy Resources Company (AER) is a technology integrator in the waste-to-energy and renewable bioenergy industry and has advised this manuscript on the utilization of waste to energy and renewable bioenergy for our technology concept; all of that industrial input is compiled in Figure 1.

Figure 1 presents the general idea of this potential trifold process in which food waste and manure are partially used as the feedstock for the anaerobic digester to produce methane. The biogas is then pre-treated to remove CO_2 before transferring to the high thermal plasma (HT plasma) gasification plant where it will undergo a gasification process in which hydrogen and fixed carbon media are produced. This HT plasma gasification plant has been developed by Laurent et al[44] and is now at a commercializing stage in the U.S. Hydrogen produced from the HT plasma gasification will be fed, together with nitrogen from the air, to the nonthermal plasma (LT plasma) developed within our group to produce ammonia. To satisfy the demand of the industry, ammonia is then integrated into the fixed carbon media and will be used as an enriching agent to increase the carbon and nitrogen content of their smart compost pellet product in soils. The pathway presented in Figure 1 is the concept we are currently developing and will need further efforts to close the loop. To make it a circular process, all streams and utilities need to be balanced based on a real ecosystem of a big region or country scale. This production scale is much about the normal factory level which will be addressed in a future article.

2 | CONCEPTUAL DESIGN AND METHODOLOGY

Figure 2A depicts a schematic illustration of the proposed process, which consists of three main reactors including an anaerobic digestion reaction for converting biomass to

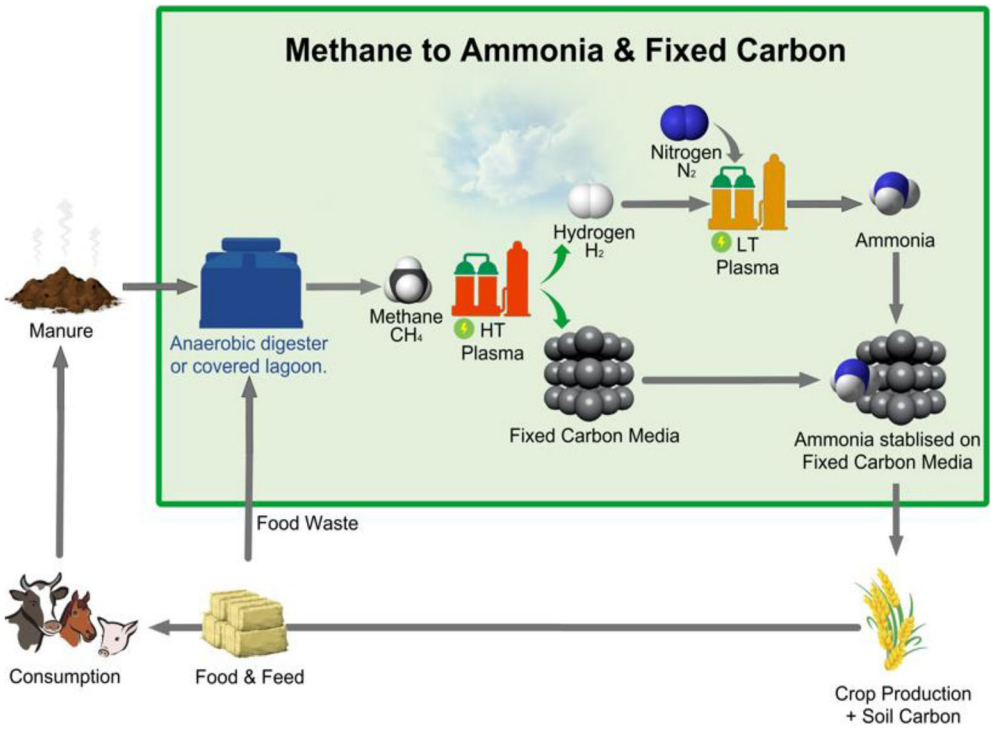

FIGURE 1 Schematic illustration of the conventional pathway for the conversion of biomass to fertilizer using anaerobic digestion, thermal plasma, and nonthermal plasma

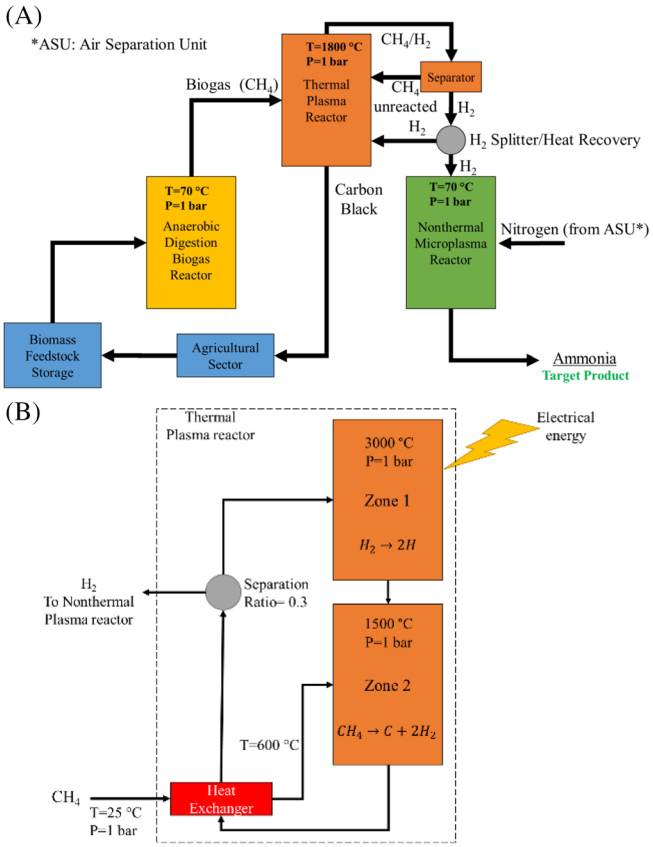

FIGURE 2 (A) Schematic diagram of the proposed process for the coproduction of ammonia and hydrogen using thermal and nonthermal plasma reactors and (B) schematic diagram of the process units for the thermal plasma reactor

biogas (methane), which is fed to a thermal plasma unit to dissociate methane into hydrogen, and it is finally converted to ammonia by a nonthermal plasma reactor for fertilizer production. The proposed process is also equipped with a steam turbine electricity production power plant to recover the waste heat from the system by producing steam and consequently, partial electricity required for the plasma reactors.

Anaerobic digestion is a chain of reactions in a reactor, in which by the help of micro-organisms biodegradable materials such as biomass are converted to biogas in the absence of reactive gases such as oxygen or steam.[47] The details of the anaerobic digestion process could be seen in Data S1.

Besides otherwise defined model cases, we also consider a real biogas plant (~200 m^2), which has been built by Peats Soil at their waste treatment site in Brinkley, South Australia. Using expired food and beverage waste collected from warehouses and retails across Australia, this plant produces by anaerobic digestion up to 10–15 m^3 biogas per day, in which methane accounts for 30% volume approximately. Several 40 m^3 HDPE (high-density polyethylene) bags are used to store the biogas, and the current plan is to utilize them as a self-supplied energy source. Yet, the future ambition, relevant for this manuscript is, to convert it by the two plasma plants to produce the first hydrogen and then ammonia. The current annual productivity is about 3.2 tonnes methane per year (15 m^3/day; 300 days; 4500 m^3). Since an upscaling by at least a factor of 10 is intended from the current pilot to production scale, we considered biomethane gas consumption of 4.8 kg/h (35 tonnes methane per year equivalent to 0.116 t/day) for this manuscript, which produces 0.21 t/day of ammonia for fertilizer production. For such systems, results showed that the system can be driven with 100% renewable energy, while 3.5 kg/h solid carbon is also produced which can bed into the agricultural sector for soil conditioning and as moisture repair. In a farther fetching demand scenario, we considered the demand side, which is to upgrade 1 kg fertilizer product with 38.5 g ammonia (3% increase in nitrogen content) at a total Peats Soil production of 200 000 tonnes compost per year. We will check if such a scenario gives enough activated carbon (coproduct in the thermal plasma process) for the loss of 40% carbon during the aerated static pile composting step in the microbe-based waste-to-fertilizer composting.

In the thermal plasma unit, the reactor provides a unique environment with a temperature so high that otherwise impossible, highly endothermic reactions become thermodynamically feasible; besides creating ions, electrons, charged and excited species. The temperature of the reactor can be as high as 3000°C, while the electron temperature reaches ~10 000 K providing a plausible environment for almost any reactions with high Gibbs free energy ($\Delta G \gg 0$) to proceed to the completion. Literature review on the use of Gibbs free energy for thermal plasma process simulation can be seen in Data S2.

The driving force for the thermal reactor is maintained with a tuneable electrical energy input (up to a dozen MW), which can be provided through renewable energy resources such as solar and wind energy. As can be seen in Figure 2B, the thermal plasma reactor has two main reactive zones. In zone 1, electric energy is converted into thermal energy through a very high-temperature thermal flow. In zone 2, methane molecules are split into solid (nanostructured) carbon and hydrogen. A heat transfer unit is also proposed to preheat the inlet methane up to 600°C, not only to reduce the thermal load of the reactor but to improve the energy performance and efficiency of the thermal plasma plant by setting a suited temperature profile for heat recovery. The produced hydrogen is then fed into the nonthermal plasma reactor to produce ammonia.

A nonthermal plasma reactor with relatively low energy consumption is the second key element of the proposed process in which ammonia is formed by a plasma-catalytic reaction of hydrogen (from the thermal plasma plant) and air. The reaction mechanism involves a variety of reactions from electron impact to surface reaction and the temperature does not play a role here; rather a complex and often not well-understood interplay with the catalyst.[48] The latter is far from well-developed and thus conversion and productivity of the nonthermal plasma typically is low and the plasma reactor units hardly have been developed larger than pilot-scale; thus, we assume this scale here and scale it up by "numbering" (of parallel reactors) alike in micro-reactor technology. Similar to a thermal plasma reactor, the nonthermal reactor is operated with large electrical energy (e.g., 30 kV peak-to-peak voltage and frequency of 50 kHz).

3 | PROCESS MODELING AND ASSUMPTIONS

Figure 3 shows the schematic diagram of the process modeled with the Aspen Plus software package together with the software package HSC Chemistry 7.0 for process flowsheet simulation of the thermal plasma unit. The energetic performance of the proposed process shown in Figure 3 was assessed for the local feedstock available at five different locations in Australia including Mandurah and Pilbara in Western Australia (WA), Streaky Bay in South Australia (SA), Moree in New South Wales (NSW), Katherine in Northern Territory (NT). For each location, the local biomass was identified and used both as a source of energy and feedstock for biogas production: grape marc for SA, mustard seeds for WA, bagasse for NT, piggery for NSW, and poultry for Pilbara, WA; with different approximate and ultimate analysis of the composition of the biomass and various lower heating values (LHV).[48] Yet, we scoped our technology not only from the regional resource-pull side but also from the local market pull: using statistical data for land and fertilizers in Australia,[49] the local ammonia-based fertilizer requirement of each location was estimated and the performance of our proposed integrated technology was assessed for each location considering all these local constraints and opportunities. The ammonia-based fertilizers include ammonia itself, urea, ammonium nitrate, ammonium phosphate, and similar derivatives.

Biomass is loaded into the anaerobic digestion and biogas is produced within an exothermic spontaneous reaction ($\Delta H < 0$, $\Delta G < 0$) at a temperature of <70°C using microorganisms. The produced biogas contains hydrogen and CO_2 thereby creating the need to separate the CH_4 to be fed into the thermal plasma plant. Notably, the proposed process is CO_2-neutral and the green CO_2 produced in the anaerobic digestion unit can be captured and sequestrated; however, this is beyond the scope of the present research. The produced methane is fed into

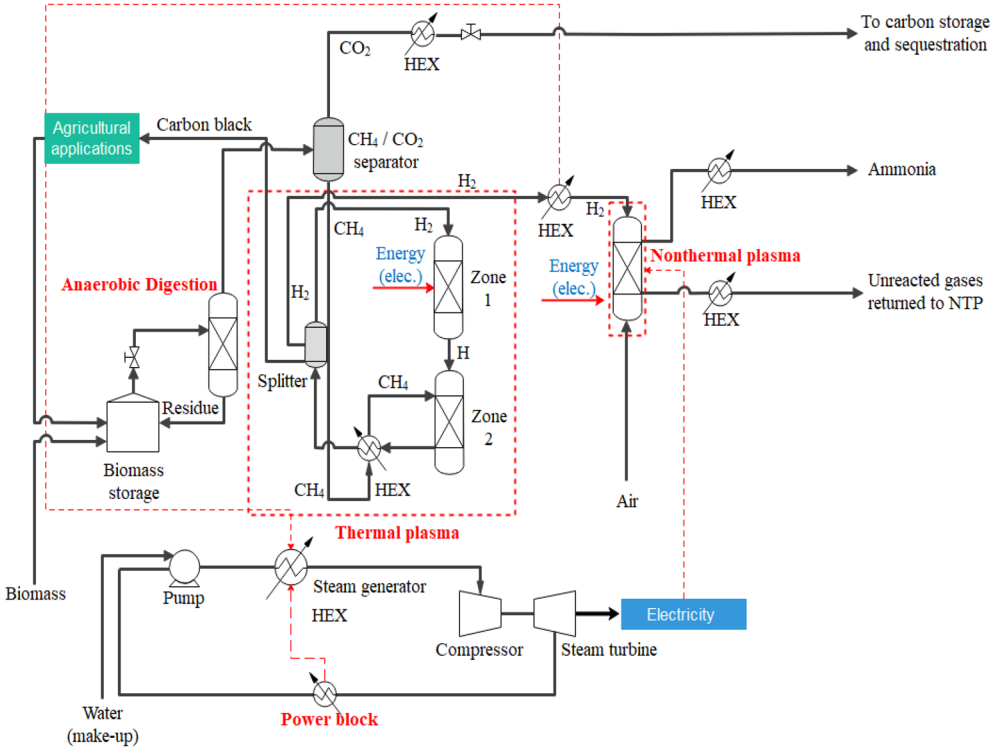

FIGURE 3 Process flow diagram of the proposed process for the production of ammonia from biomass using combined high- and low-temperature plasma technology

the thermal plasma reactor to be decomposed into hydrogen and carbon. The thermal plasma reactor has two reacting zones.[50] Methane is fed into zone 2 to be dissociated into solid carbon and hydrogen via the main reaction of $CH_4 \rightarrow C + 2H_2$. The outlet from the biogas reactor is fed first into zone 1, where a heat exchanger preheats the inlet stream of methane and thereby improves the energetic performance of the unit. By doing so, the temperature of the methane gas increases from ~60°C to 600°C. This reduces the thermal load of the reactor. Notably, the upper threshold for the preheating temperature of methane is 700°C to avoid cracking methane in the pipes. Hence a buffer temperature of 100°C with a pinch point of 10°C was considered for the preheating heat exchanger. A heat recovery rate of 77% was obtained for the heat exchanger by the Aspen modeling, meaning that the stream preheating stage can avoid a large heat loss by returning the heat to the reactor. Then the cold product stream is fed into a separator, in which solid carbon is separated from the product stream and a fraction of hydrogen is fed into zone 2 to produce hydrogen radicals through the reaction $H_2 <=> 2H$ via electrical energy. The split into two serial reaction zones increases the chemical yield of the thermal plasma reactor.[44,50]

The fed hydrogen to the nonthermal plasma reacts with the nitrogen brought by air to the reactor to produce ammonia, and the chemical reaction is the same as for the Haber–Bosch process, yet the latter is a purely catalytic process without plasma and needs instead high temperature and high pressure. The nonthermal reactor has a temperature of ~130°C and operates at atmospheric pressure, thus would not be competitive under equilibrium conditions. Such plasma acts in a nonequilibrium way, and the opportunities of that are theoretically hardly unknown; alone for the reason of the many hundreds of reactions happening and that each different plasma type influences them differently. Yet one seems to be clear: the enhancement of surface reactions of activated species on the catalyst is likely a key to intensify. The relatively large volumes of low-temperature plasma reactors, as compared to diffusion distances and the short-living times of plasma-reactive species, allow only for low conversion, as those species do not reach the catalyst, and the literature is full of studies documenting this fact.[51,52] To address this challenge, one potential option is to use a series of reactors to produce ammonia at the desired level, which stepwise may increase the conversion and thus productivity. Hence, in the present simulation, the nonthermal plasma is considered as one operational unit, which is a modular system with a series of nonthermal plasma reactors. The outlet from the nonthermal plasma reactor is fed into a separator to split the produced ammonia from unreacted hydrogen and air. Also, a design specification was defined to regulate the inlet gas stream of the process such that the outlet hydrogen from the nonthermal plasma is minimized. Notably, the LHV of hydrogen is 119 MJ/kg, thereby showing that the unreacted hydrogen can carry a large amount of energy from the system. Hence, the optimization of the operating conditions was carried out to avoid chemical and energetic losses. Using two heat exchangers, the outlet streams from the thermal plasma reactor were cooled and the recovered heat was employed to produce steam at 410°C and 30 bar. A steam turbine was used to produce electricity and return a fraction of waste heat to the process plant. This was done to improve the energetic performance of the system and to supply the reactor energy demands partially. The produced electricity was dedicated to the nonthermal plasma reactor(s).

To calculate the values for enthalpy of reaction and also the change in the Gibbs free energy of the reactions in the process, Equation (1) was implemented:

$$\Delta M_{\text{rxn}} = \sum_{\text{prod}} \Delta M_i^f(T) - \sum_{\text{react}} \Delta M_i^f(T). \tag{1}$$

Here, "M" stands for the enthalpy of reaction (H) or change in the Gibbs free energy of the reaction (G) for species i. Notably, the subscripts "rxn", "react" and "prod" are abbreviations for reaction, reactants and products of each reactor, respectively.

To evaluate the exergy portioning of the system, exergy efficiency (χ) was defined with Equation (2):

$$\chi = \frac{\dot{n}_{NH_3} \times LHV_{NH_3} + \dot{n}_{H_2} \times LHV_{H_2}}{\dot{n}_{\text{feed}} \times LHV_{\text{feed}}}. \tag{2}$$

In this equation, $\dot{n}$ is the flow rate of each stream, LHV is the value of the lower heating value of ammonia and hydrogen, which are 18.6 MJ/kg and 119.9 MJ/kg, respectively. Also, the total thermodynamic efficiency, considering 3% of inlet thermal energy as a heat loss to the environment. is defined as follows:

$$\eta_{\text{th}} = \frac{\left[\sum_{i=1}^{n} n_i \times \Delta H_i\right]_{\text{out}} + W_{\text{power block}} - W_{\text{pump}} - Q_{\text{loss}}}{\sum Q_{\text{net},R_z} + \left[\sum_{i=1}^{n} n_i \times \Delta H_i\right]_{in}} \tag{3}$$

Here, $W_{\text{power block}}$ is the thermodynamic work produced by the steam turbine and the W_{pump} is the amount of energy consumed by the pump to produce a high-pressure water stream for the power block system. Likewise, Q_{loss} is the heat loss to the environment calculated

based on the equation given in the literature which is ~3% of total input. The self-sustaining energy fraction of nonthermal plasma is also defined in Equation (4) which is used to estimate the portion of energy to be produced by the power plant:

$$\in = \frac{W_{\text{elec.}}\,[\text{kWh}]}{W_{\text{NTP}}[\text{kWh}]} \tag{4}$$

In this equation, W is the electrical energy, and "NTP" and "elec." stand for nonthermal plasma and electrical energy produced by power block, respectively.

To calculate the output energy of the solar photovoltaic system, the following equation is employed:

$$E = A_{\text{PV}} \times r_{\text{PV}} \times H_{\text{ann.}} \times \text{PR} \tag{5}$$

Here, E is the energy produced by a solar photovoltaic system (kWh), and we will later justify the consideration of photovoltaic energy; with A_{PV} being the total solar panel area required to maintain the demand, r_{PV} is the solar panel yield, $H_{\text{ann.}}$ is the annual average of radiation received on tilted solar panels and *PR* is the performance ratio that accounts for any losses from the solar panel system, which is 0.5 (worst case scenario and 0.9 for the best-case scenario). Otherwise, a value of 0.75 is considered. There are different losses associated with the use of solar panels, including inverter losses (6–15%), temperature losses (5–15%), cables and connector losses (1–3%), AC cable losses (1–3%), shadings up to 40% depending on the location, and losses due to the dust and debris (2%). In the present study, an inverter loss of 8%, temperature loss of 8%, DC and AC losses of 2%, and shading loss of 3% and loss due to the dust of 2% were considered in the model.

To conduct the simulations, the following boundary conditions and assumptions are taken as seen in Data S3.

4 | CHEMICAL REACTIONS AND PLASMA CHEMISTRY

The equation for the reaction for converting biomass into methane via the anaerobic digestion process is given in Table 1. As can be seen, the reaction is slightly exothermic and due to the activity of the microorganisms, the temperature is limited to <70°C, although there are cases in which the anaerobic digestion process can be done at higher temperatures but at higher risks of thermally decomposing the microorganisms.

Table 2 expresses the main elemental reactions occurring in the thermal plasma reactor in reaction zones 1 and 2. As can be seen, some of the reactions such as 2, 3, and 6 have a temperature barrier and likely may not run or only slowly at the low temperature of the plasma. For example, the homolytic splitting into radicals via the elemental reaction 2, the temperature of the reactor should be higher than 3000°C. However, the other elemental reactions may be effective at a temperature <2000°C. Therefore, for reasons of energy efficiency, it is mandatory to divide the thermal plasma reactor into two reacting zones, one with a minimum temperature of 3000°C referred to as "zone 1" and the other one with a minimum temperature of 1500°C referred to as "zone 2." Also, some of the reactions in Table 2 are endothermic, while some are exothermic. Thus, the co-existence of

TABLE 1 The reaction occurring in the anaerobic digestion reactor for the biogas production from biomass

No.	Reaction	ΔH_{rxn}, kJ/mol	ΔG_{rxn}, kJ/mol	Temperature,°C
1	$C_xH_yO_z(s) \rightarrow \frac{x}{2}CO_2(g) + \frac{x}{2}CH_4(g)$	< 0	Exothermic ($\Delta H < 0$)	<150

Note: The values for *x*, *y*, and *z* strongly depend on the structure and composition of the biomass.

TABLE 2 Main elemental reactions occurring in the thermal plasma reactor for the hydrogen production through biogas cracking

No.	Reactions	Zone	ΔH_{rxn}, kJ/mol	ΔG_{rxn}, kJ/mol	Temperature,°C
2	$2CH_4(g) \rightarrow 2CH_3(g) + H_2(g)$	2	155.2	−9.2	1500–6000
3	$2CH_3(g) \rightarrow C_2H_6(g)$	2	−382	−250	500–6000
4	$CH_3(g) + C_2H_6(g) \rightarrow CH_4(g) + C_2H_5(g)$	2	−29.9	−34.1	100–6000
5	$2C_2H_5(g) \rightarrow 2C_2H_4(g) + H_2(g)$	2	−103	−150.4	300–6000
6	$CH_4(g) \rightarrow C(s) + 2H_2(g)$	2	87.4	−5.5	700–6000
7	$H_2(g) \rightarrow 2H(g)$	1	123.5	−2.5	3000–4000

generating temperature in the reactor with the consumption of energy leads to a complex energetic performance of the thermal plasma, by superposition of simple energy balances. Hence, a thermochemical equilibrium analysis was used to understand the energy flow of the system.

Having that background at first principles, it is possible to make a gross prediction of the integrated reactor performance using the distinct local factors. In this sense, Table 3 expresses the detailed approximate and ultimate analysis of the biomass feedstock identified for each of the chosen five locations in Australia together with the lower heating value (LHV), composition and quantity of moisture available in the biomass. It is worth mentioning that the LHV of the feedstock affects the performance of the process due to the change in the input chemical exergy value to the chemical plant. As mentioned in the list of boundary conditions and assumptions, it is assumed that the sulfur and other impurities are accumulated in the residue and are returned to the biomass storage. Hence, the analysis here considers no SO_x is formed in the system.

5 | RESULTS AND DISCUSSION

5.1 | Project feasibility

5.1.1 | Thermochemical equilibrium analysis

As previously discussed, the thermal plasma reactor requires a high temperature to proceed with the reaction toward the equilibrium state. We propose a two-zone reactor over one equilibrium unit to decrease the energy demand and also the efficiency of the process. Figure 4 presents the calculated variation on the temperature of the change in the Gibbs free energy of the reactions in a one-zone thermal plasma reactor. As perceived from the Figure, at a point above 2000°C, the Gibbs free energy turns to $\Delta G < 0$ for all reactions, meaning that the chain of the reactions given in Table 2 is thermodynamically feasible to occur in the reactor. However, for a region between 100°C and 1500°C, most of the reactions have $\Delta G > 0$, which means that the reactions are not spontaneous and require an external driving force to proceed, which could be pressure or any passive technique such as electromagnetic forces. This would increase the energy

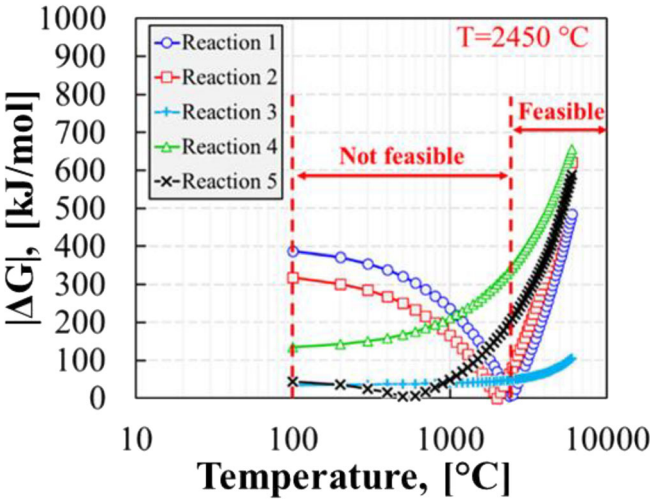

FIGURE 4 Variation of the calculated Gibbs free energy of the reactions with temperature for the one-zone thermal plasma reactor

TABLE 3 Proximate and elemental analysis of the biomass used in the present research[53]

	Grape marc (SA region)	Mustard seed (WA region)	Bagasse (NT region)	Piggery (NSW region)	Poultry (WA region)
Proximate analysis (%)					
Moisture^{wb}	10	11.8	12.8	12.7	39.7
Fixed carbon^{db}	31.1	17.14	11.88	19.12	–
Volatile matter^{db}	55.6	70.1	84.51	54.91	–
Ash^{db}	13.3	15.4	3.61	13.27	10.58
LHV^{db}	18.02	16.25	17.27	14.47	15.77
Elemental analysis^{db} (%)					
C	42.2	41.82	48.19	38.12	24.83
H	3.5	8.35	5.65	3.65	3.77
O	37.7	40.01	42.33	29.25	17
N	3	0.36	0.14	2.16	3.67
S	0.3	0.18	0.08	0.42	0.3

Abbreviations: db, dry basis; LHV, lower heating value; wb, wet basis.

demand of the thermal plasma reactor to operate at the equilibrium point.

To avoid that, as discussed in the previous section, the operation of the reactor was amended such that the two reactive zones are formed in the thermal plasma plant. In the related thermal plasma reactor, one reactor with a high temperature is responsible for ionizing the hydrogen and exciting the species to bombard the methane (CH_4) in zone 2. By doing so, the thermal efficiency of the system is enhanced from 40 to 13.3 kWh/kg H_2. Also, the minimum operating temperature of the reactor (temperature of the gas bulk) decreases from 2450°C to ~1500°C, which lowers the sensible heat required for the operation of the reactor.

5.1.2 | Thermal energy

Figure 5 presents the variation of the thermal energy of the thermal plasma reactor with the temperature of zone 1 (Figure 5A) and zone 2 (Figure 5B). For better understanding, a parameter is defined as the ratio of the difference in the thermal energy of reacting zones to the thermal energy of a given reacting zone. As can be seen, for zone 1, with an increase in the temperature, the ratio (thermal energy deviation) decreases, which is associated with the decrease in the enthalpy of reaction (exothermic dissociation of $H_2 \rightarrow 2H$) in zone 1. However, in zone 2, with increasing the temperature, the ratio approaches 1 showing that the reactors reach isothermal conditions. Such an operating condition is more plausible, as the exergy annihilation between the zones of the reactor decreases and the ratio equals 0.99 at $T > 3000$°C. Hence, the best-operating conditions can be obtained at $T = 3000$°C, in which the ratio approaches 1 and the exergy annihilation between reactors is minimized. Also in this condition, the specific enthalpy of the hydrogen production reaches 13.3 kWh/kg H_2, which is 33.2% of the total specific enthalpy obtained for a one-zone thermal plasma reactor (40 kWh/kg H_2).

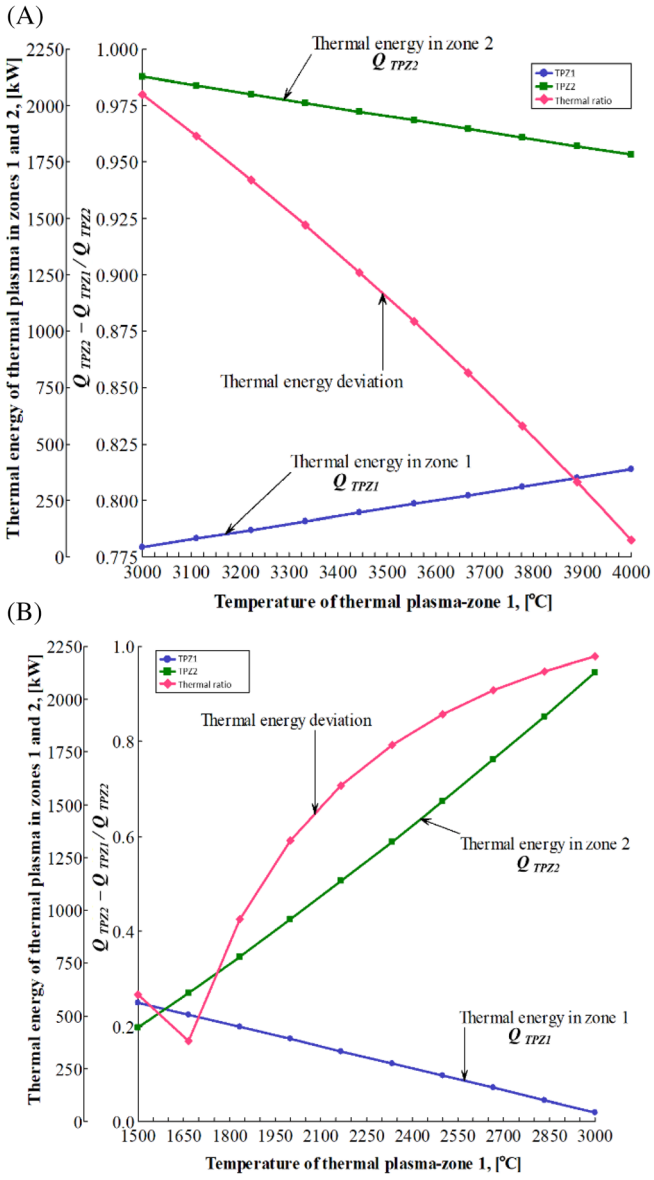

FIGURE 5 Calculated variation of thermal energy of the two-zone thermal plasma reactor with temperature

5.1.3 | The temperature of the thermal plasma reactor

In Figure 6, the variation of the mole fraction of the products with the temperature of the thermal plasma at isothermal conditions is shown. As can be seen, at $T > 2500$°C, the evolution of the mole fraction of hydrogen H(g) decreases, which in turn decreases the thermal demand of the reactor. For example, at $T = 1500$°C, the mole fraction of H(g) is zero, while reaching 0.3 at $T = 3000$°C. for the same temperature range, the mole fraction of H2(g) decreases from 0.7 to ~0.42. Notably, once H(g) is formed, it is transported to the reacting zone 2, which promotes the conversion of the methane toward the equilibrium point, and lowers the thermal energy in zone 1 by transporting it to zone 2. Thus, the operating temperature of the plasma reactor in zone 1 should be controlled between 3000°C and 4000°C to maximize the evolution of H(g), and the temperature of zone 2 should be regulated between 1500°C and 2500°C.

5.1.4 | Exergy portioning in the system

Figure 7 presents the variation of the exergy efficiency with the temperature of reacting zones of the thermal

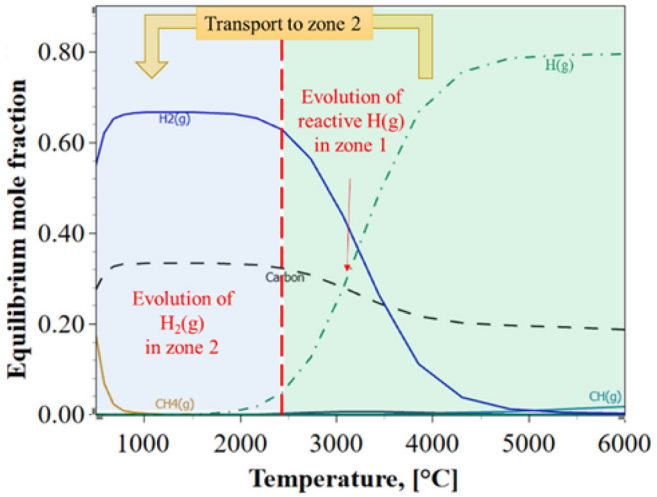

FIGURE 6 Variation of the mole fraction of the components with temperature in the thermal plasma reactor (TPR)

plasma reactor. As can be seen from Figure 6A, the temperature of zone 1 does not affect the total efficiency and the exergy partitioning in ammonia, while it slightly increases the self-sustaining energy fraction and exergy destruction of the system. This is because by increasing the temperature in zone 1, the temperature difference between the two zones increases and results in an increase in the unit's exergy annihilation. However, with increasing the temperature of zone 2, the total efficiency of the system increases, which is attributed to the increase of the enthalpy of the endothermic reaction $CH_4 \rightarrow C + 2H_2$. As shown in Figure 11B, the self-sustaining energy fraction is ~0.7 at $T = 3000$ C, which can reach 1.0 by increasing the temperature of the reaction zone 1 from 1500°C to 1300°C (see Figure 8).

5.1.5 | The pressure of the thermal plasma reactor

Figure 8 shows the calculated dependence of the mole fractions of the products in the thermal plasma reactor on the pressure of the system. As perceived, the mole fraction of hydrogen is slightly enhanced with the increase in the pressure of the reactor. However, by pressurizing the system, the operation of the process becomes more complex, which also adds to the cost and maintenance expenditures associated with the operational units. It is worth mentioning that the pressure of the reactor does not affect the rate of production of solid carbon, thereby maintaining a constant rate of solid carbon production in the system. As can be seen, the mole fraction of H_2 (g) is very slightly enhanced from ~0.62 to ~0.66 by increasing the operating pressure from 1 to 30 bar. At

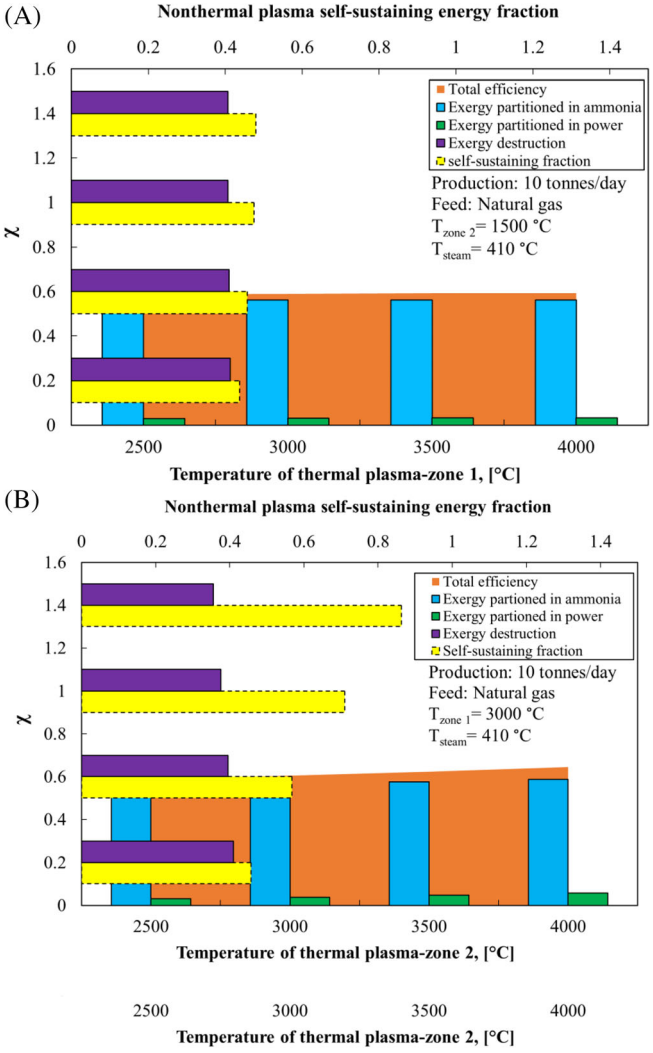

FIGURE 7 (A) Variation of the exergy partitioned in the system versus the temperature of a thermal plasma reactor in zone 1 and (B) variation of the exergy partitioned in the system versus the temperature of a thermal plasma reactor in zone 2

$P > 30$, pressure does not affect the mole fraction of the species.

5.1.6 | Mechanical work production

Figure 9 shows the variation of the self-sustaining energy fraction of the nonthermal plasma reactor with the temperature of the thermal plasma reactor at a varying inlet pressure of water to the steam generator. As can be seen, with an increase in the temperature of the thermal plasma reactor, the quantity of the work produced by the power plant increases such that the self-sustaining energy fraction reaches ~1 at $T = 3000$°C. This means that the electricity required for the Nonthermal plasma plant can be fully supplied by the electricity produced in the power

block. For example, at $T = 1500°C$, at $P = 60$ bar, the self-sustaining energy fraction is ~0.54, reaching 1 at $T > 2600°C$. For the same temperature range, at $P = 20$ bar, the self-sustaining fraction increases from 0.44 to 0.85. Hence, there is a need for an external energy resource to provide the rest of the required energy. Notably, a linear trend is observed between the temperature of the thermal plasma and the self-sustaining energy fraction. Hence, a large thermal plasma plant can be advantageous not only to provide more hydrogen but also to promote the self-sustaining energy fraction of the nonthermal plasma plant.

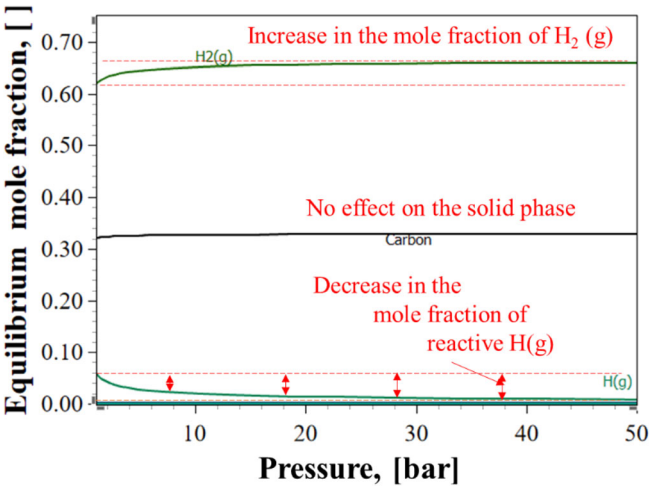

FIGURE 8 Variation of the mole fraction of the components with pressure in the thermal plasma reactor (TPR)

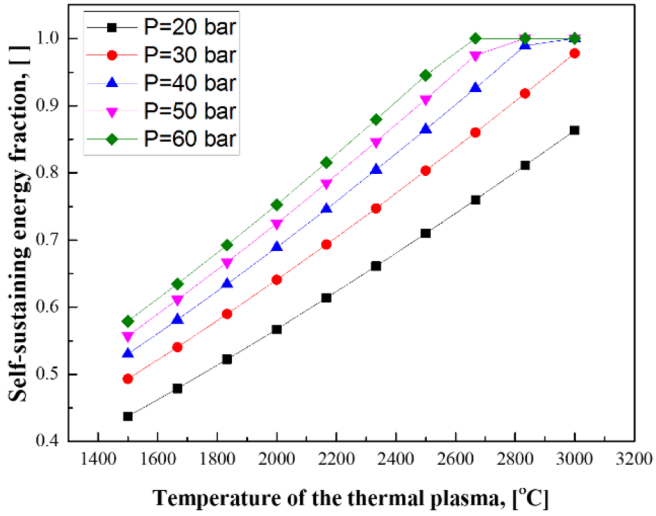

FIGURE 9 Variation of the self-sustaining energy fraction to with the temperature of the thermal plasma unit for supplying the energy consumption of the nonthermal plasma reactor

5.2 | Suitability to local, resilient, and self-sufficient production

In the following sections, it is aimed to answer if the system can show the desired features of industry transformation, which are local adaptability, self-sufficiency, and resiliency. It is considered that resiliency is not a quantity on its own, but rather developing and interpreting the system's capability as related to local adaptability and self-sufficiency toward a holistic concept with reference to a specific supply-chain and business model; as given in the introduction.

5.2.1 | Local adaptability

Resource flexibility using local feedstock

In Figure 10, the variation of the exergy efficiency with the production scale is depicted for the five chosen locations in Australia, when using local biomass as a feedstock. As perceived from the Figure, the efficiency of the system decreases with an increase in the production scale of the plant. This is because the production of ammonia is limited by the capacity and yield of the nonthermal plasma reactor. Hence, for the large production scale, there is a need to develop high-yield reactors by finding a proper catalyst to increase the yield aiming at removing this chemical barrier. As can also be seen, the NSW site with piggery as biomass shows the largest exergy efficiency in comparison with the other locations, followed by Pilbara (WA) and Mandurah (WA). This is because, for a similar yield, piggery has a relatively low LHV value and plausible hydrogasification conversion, resulting in larger exergy efficiency. However, with an increase in the production scale, for example, 588.2 t/day, plausible locations are Moree (NSW), followed by Streaky Bay (SA) with a production scale of 260 t/day. It is worth mentioning that the lower heating value of the biomass also affects the efficiency of the system. For biomass such as grape marc and bagasse, the LHV value is relatively large, however, the conversion of biomass to biogas is limited as the content of volatile material is relatively lower than other biomass feedstock. Apart from that, the ash content, which limits the mass transfer, is relatively high for this type of biomass feedstock, thereby reducing the efficiency of the plant. For the real-life data collected from Peats Soil Company in SA, with a production scale of 0.2 t/day, the exergy efficiency of 0.58 was calculated which is competitive to large-scale productions, for example, 409.9 t/day. This shows that plasma technology is flexible to the scale of production. Table 4 represents the production scale, solar area and number of wind turbines

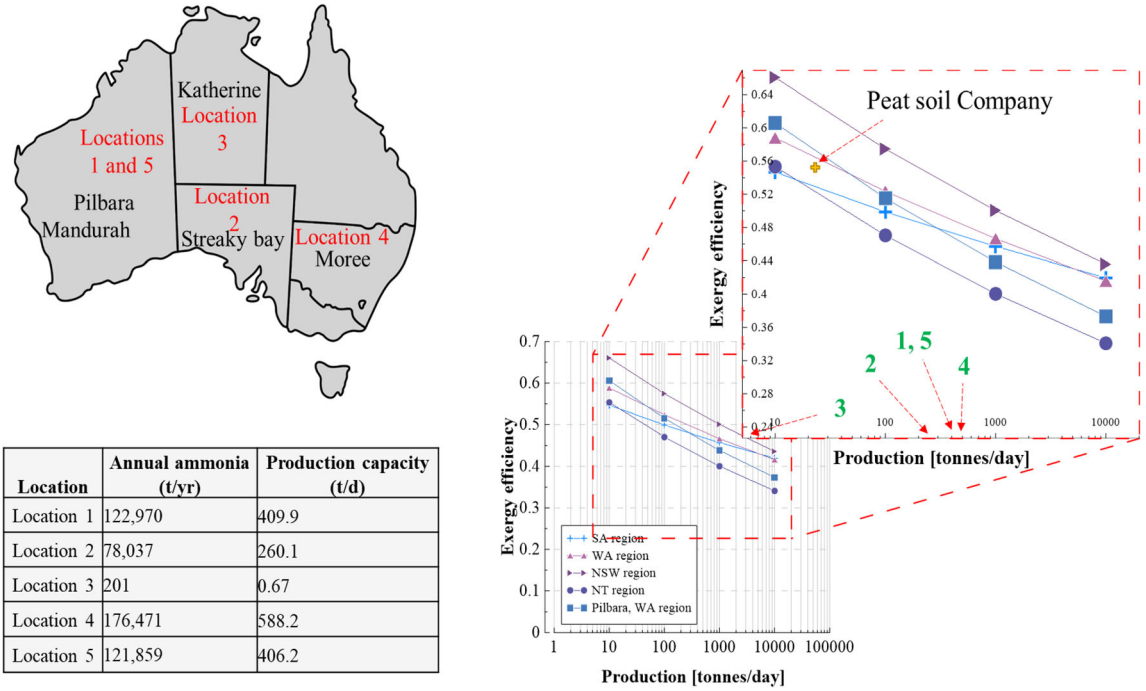

Location	Annual ammonia (t/yr)	Production capacity (t/d)
Location 1	122,970	409.9
Location 2	78,037	260.1
Location 3	201	0.67
Location 4	176,471	588.2
Location 5	121,859	406.2

FIGURE 10 Variation of the exergy efficiency of the system with the temperature calculated based on real-life data at the five chosen agricultural locations for the production of ammonium-based fertilizers based on the local needs

TABLE 4 Summary of the required fertilizers at the five chosen agricultural locations, considering the type of the biomass, and renewable energy share typical for each location

Location	Annual demand of NH_3 (tonnes/a)	Production capacity[a] (tonnes/day)	Solar field, (km^2)[b]	Wind turbine[c]
1	122 970	409.9	4.04	237
2	78 037	260.1233	2.6	179
3	201	0.67	0.03	1
4	176 471	588.2367	5.8	321
5	121 859	406.1967	4	236

[a]Based on the capacity factor of 0.85, and statistical data for ammonia consumption in the locations.
[b]Estimated for January.
[c]For wind speed >6 m/s in July.

required to hybridize the system with renewable energy resources.

Production capacity, defined by exergy efficiency

We like to add two plausibility checks for the economic validity of our integrated process concept. The first one given here is based on thermodynamics (exergy), meaning the efficiency of using energy to make the product. The second one given below is based on process plant footprint (area) and the number of process plant units; assuming a pure numbering-up from a size that is considered to be reasonable or even already industrially proven.

As can also be seen from Figure 10, the exergy efficiency decreases with the increase in the production scale, which is due to the increase in the input energy of the system while the yield of the anaerobic digestion system is constant. To address that, there is a need to develop reactor technologies, which can offer higher yield at a larger production scale. Considering the exergy efficiency of 0.21 as a "threshold for useful exergy efficiency" defined in the literature,[54] for all geographical locations and production scales, the system is still economically viable as the exergy of the process is well above 0.3.

TABLE 5 The calculated ammonia equivalent and amount of fertilizer required for different locations studied in this study

Parameter	Ammonia equivalent	Urea	Ammonium phosphate	Ammonium sulfate	Ammonium nitrate
MW, (g/mol)	17	60.06	149.09	132.1	80.04
Ammonia ratio	–	0.2831	0.114	0.1287	0.2124
Location 1, (t/a)	122 970	286 772	244 644	63 910	26 696
Location 2, (t/a)	78 037	166 419	212 778	27 739	14 582
Location 3, (t/a)	201	472	543	18	12.7
Location 4, (t/a)	176 471	470 112	299 438	33 477	23 250
Location 5, (t/a)	121 859	285 550	244 644	60 470	25 180

Abbreviation: MW, Molecular weight.

TABLE 6 The calculated land area and number of the proposed process plants at the five different Australian locations based on production scale given in Table 4

Location	Land for bio-mass plant (km^2)	Land for TP plant (km^2)	Land for NTP (km^2)	Total land[a] (km^2)	No of biomass plant[b]	No of TP[c,d]	No of NTP[d,e]
1 (WA)	32.1	0.21	0.0012	32.310	214	8	12
2 (SA)	20.4	0.13	0.0008	20.530	136	6	8
3 (NT)	0.15	0.0003	0.0001	0.151	1	1	1
4 (NSW)	46.2	0.31	0.0018	46.512	308	11	18
5 (WA)	31.8	0.21	0.0012	32.011	212	8	12

[a]Considering 20% of the total required area as a space between plants.
[b]Each biomass plant requires an area of 150 000 m^2 to produce 500 kg/day (approximately 1000 m^3/day) of biomethane.
[c]Each TP plant with capacity of 16 kt/a requires 40 468 m^2 of land.
[d]renewable energy share >0.85.
[e]Each NTP plant with capacity of 10 kt/a requires 100 m^2 of land.

Production capacity, defined by the number of reactor/plant units and plant footprint

In Table 5, the ammonia equivalent is calculated, which needs to be produced to generate all ammonia-based fertilizers used in Australia (including ammonia itself). Knowing the chemical reaction equations of the conversion of ammonia to these, the total ammonia equivalent can be calculated, using the real-life data from each geographic location. This fertilizer mix includes urea, ammonium phosphate, ammonium sulfate, and ammonium nitrate. It is assumed that the conversion of the reaction from ammonia to the different types of fertilizers is 90%. This information was used to obtain the footprint of the proposed plant and the number of reaction/plant units. This projection needs several assumptions.

For the biomass plant, a 60% gas share of biomethane in the biogas is assumed. A factor of 3 in plant capacity is assumed, as the technology has intrinsic limits and only limited process optimization can be applied. Literature review shows that a biomass plant of 500 kW will require an area of 8000 m^2 approximately.[55] Fortunately, there is a chance to upgrade the capacity of the biomass plant if a central collection site is designed and constructed. One of the largest biomass plants in Australia, the Uleybury landfill site, could produce up to 650 m^3 biogas/h.[56] Recent reports about an industrial plant in New Zealand give hope for a reduction of the land use of biomass plants;[57] which now is prohibitively large and Table 6 shows this clearly outpaces the two other plants.

The performance of the thermal plasma plant was taken as received from literature reports. It is assumed to be on a high and final technology readiness level. The performance of the nonthermal plasma (NTP) plant is far from that. We refer to the statement of Evonik Industries that a 2% yield-performance can deliver 1 kt/a in their NTP container plant, and our experiments are not far from this. As in literature higher yields have been reported and plasma catalysis is considered as a prime process intensification enabler, it is assumed reasonably to apply a factor 10 in the assessment of Table 6.

On this background, Table 6 shows the proposed footprint (area) and the number of industrial production plants for the three process stages and their total value, satisfying the ammonia production scale needed for

producing the fertilizer mix. The latter were recalculated from the data using the stoichiometric ratio and assuming an average conversion of 90%.

The data shows, and not surprisingly, that while the thermal plasma plants—rated by their mere numbers—suits the scale of industrial fertilizer production (which is mega-scale), whereas the two other processes—the biomass and nonthermal plasma plants—are not yet ready for that concerning a production scale of a sub-national level. Any numbering-up of plants/reactors above 10 and area above 0.5 km^2 is questionable, and thus substantial technology development is demanded.

Remarkably, the land use of the nonthermal plasma plants is low and commercially competitive, as we assumed it profits from the use of compact container technology and process intensification; this is exactly the scope within it has been developed. The high number of nonthermal plasma plants is unfavorable external numbering-up and may be reduced by internal numbering-up of reactors and scale-up of separation units.[30,58]

Taking all those optimistic assumptions, the predicted number of plants would be: About 10: 1: 2 number of plants for biomass: thermal plasma: nonthermal plasma plants, respectively. That ratio seems reasonable, and may give chance for further optimization.

Thus, today's process technology of all three plants could satisfy the demand of the Northern Territory region and any 10-times equivalent of it; it may satisfy the fertilizer on a regional level; for example, for a farmers collective needing a few 1000 t/a. Our proposed production technology as of today, is ready for a collective of about two farmers who are growing crops on a total land of 30 000 ha approximately in all of Australia's regions. Within this region, the approach is resilient and flexible against various production scales. Anything above that scale, needs a reinvestigation of the laboratory technology, to give process intensification in the lieu of above-mentioned concrete improvements. The nonthermal plasma technology, for example, is just at its beginning and has been improved over the last decade. It can probably improve toward a capacity of one order of magnitude and more.

5.2.2 | Self-sufficiency

Renewable energy: hybridization with a solar photovoltaics

Figure 11 represents the variation of the renewable energy share with the months of the year for the proposed system at the five different geographical locations in Australia. As can be seen, the highest renewable

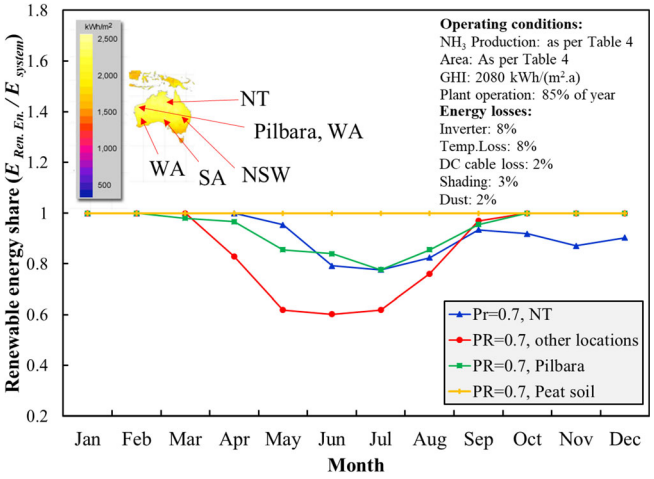

FIGURE 11 Comparison between the solar photovoltaic share calculated based on real-life data for the chosen five different geographical locations in Australia

energy fraction is seen from January to March in the Australian summer, when the solar irradiation is the highest. As shown, there is no difference between the energetic performances of the system in all locations as the solar radiation can provide sufficient energy demand to supply the electricity required for the plant. However, from April to September, the solar irradiation is reduced due to the change in the angle of the sun, and hence the renewable energy fraction decreases reaching from 0.91 to 0.77 for the NT site and from 0.79 to 0.6 for the other locations. For Pilbara in WA, the energetic performance of the system still is relatively high as the amount of irradiation in this geographical location is >2200 kWh/m^2 per year. It is worth mentioning that there is a potential to hybridize the system with an electrical storage unit particularly for the period from October to March in all locations, which would the energetic performance of the system. However, this is beyond the scope of the present study and might be investigated in ongoing works by our group. Notably, the solar panel yield considered in the simulation was 15%, thereby developing more efficient solar panels will, in turn, improve the energetic performance and renewable energy share of the system as well.

Figure 12 represents the variation of the renewable energy fraction with the area of the solar photovoltaic field for different locations in Australia at PR = 0.5. As can be seen, considering all the losses in the system and solar field area of ~10 km^2, the renewable energy fraction approaches 1. This means that the system can self-sustain with a renewable energy source such as solar photovoltaics providing that electrical energy storage is used in parallel to accumulate the extra energy and to avoid electrical energy purged from the system. This, of course, requires a huge storage system and infrastructure

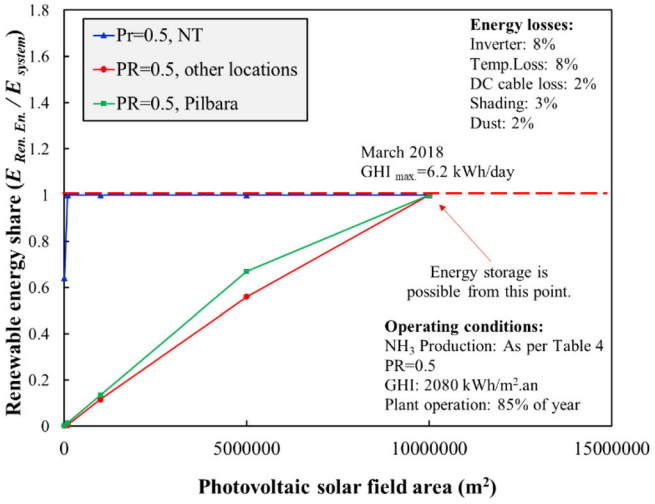

FIGURE 12 The calculated dependence of the photovoltaic solar energy share value on the solar field area for different locations based on the real-life data in Australia

and a robust techno-economic assessment. Also, process intensification might be a potential solution to reduce the area required for the development of the solar photovoltaic farm. For the present research, the yield for the solar panel was 0.15, however, by developing high-yield solar photovoltaic systems including efficient panels, storage and inverters, the required area can be reduced.

Renewable energy: Hybridization with wind energy

In Figure 13, the potential hybridization of the proposed system with wind energy is investigated. Figure 13 represents the variation of the renewable energy fraction with the number of wind turbines required to supply the energy demand of the system. In Figure 13A, the performance curve of the 1.5 MW wind turbine is shown. As can be seen, the performance of the wind turbine is relatively low at wind speeds <15 m/s. Since the wind data for the five chosen locations are mostly <10 m/s, the turbines cannot work at their maximum nominal capacity, which in turn would require the installation of more wind turbines to compensate for the wind speed. As can be seen in Figure 13B, the minimum number of wind turbines, which can fully cover the energy demand of the system is 1 for the NT site, >350 for other locations and 250 for Pilbara in WA. Thus, it depends much more on the specific location than given for the solar panel farms. Notably, the efficiency of the turbine is also another key parameter affecting the number of wind turbines to be installed and also the capital investment required for the wind turbines. For example, for Pilbara, for the low-efficiency case (0.1) the minimum number amounts to 400 wind turbines and for the high-efficiency case (0.3) only 250 wind turbines are required to fully cover the

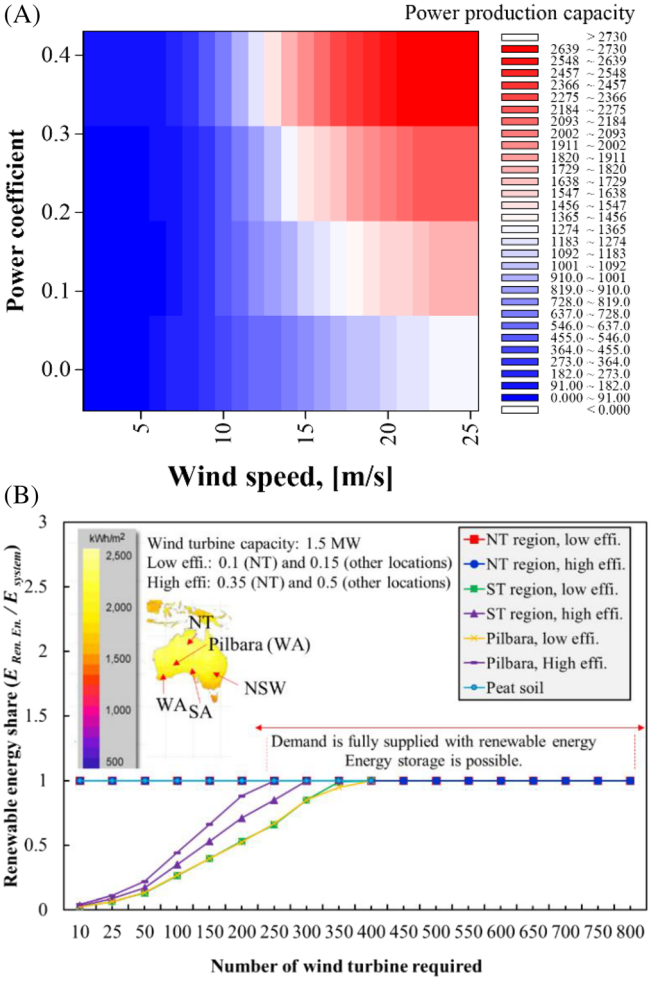

FIGURE 13 (A) Performance diagram and power coefficient for the wind turbine based energy generation considered in the model extracted from literature[1] and (B) the calculated dependence of the wind energy share with the number of turbines required to supply the energy demand of the system in the five chosen locations based on the real-life data in Australia

energy demand of the system. As a technological upgrade, electrical storage can be used to store the electrical energy, when wind speed is above 10 m/s, and be used when the wind speed is not high enough. Amongst the locations assessed in Australia, Pilbara shows great potential, since there the proposed system can be hybridized with a wind farm to produce the required energy demand for the plasma reactors.

5.2.3 | Resiliency

Holistic view in terms of the industrial transformation

In the two previous sections, we have already assessed indirectly the resiliency of the proposed systems, when discussing their local adaptability and self-sufficiency, in

TABLE 7 Detailed information on the local, resilient and self-sufficient performance of the proposed process in view of a holistic resiliency

Parameter	Feature in the proposed system	Quantitative/qualitative results
System capacity		
Geo-economics and fertilizer demands	The proposed system shall offer a thermodynamic potential to be used at any geographical location and is adapted with the local biomass and renewable energy available.	The system was assessed based on real-life data collected for wind, solar, type of biomass and fertilizer demands of various geographical locations in the states of South Australia, Western Australia, Northern Territory and New South Wales. Based on the fertilizer consumption of each location, the system can be tuned and the energetic performance turned out to be resilient at each, being able to be tuned according to the local needs and end-user requirements.
System response	The system shall have a quick response for changing parameters to generally increase flexibility, yet most desirably for changing the productivity, while operating with one reactor.	It is proposed that the thermal reactor shall use two reaction zones, with two different temperatures, which are responsive to the residence time of micro- and nano-seconds. This allows altering the production rate through increased rate of H(g) radical formation.
Scale of production	The proposed system shall be flexible against the production scale and the simulations of this article showed that number of nonthermal plasma reactors can be identified based on the production scale.	It is predicted that the system could operate at 0.2 t/day (Peats soil company) to 624 t/day (in Western Australia), with large variation based on the local demand and end-user requirements. The productivity of the thermal plasma reactor can be changed elegantly by the above-mentioned system response; the productivity of the anaerobic digestion and the nonthermal plasma reactor, can only be changed by scale-up, process intensification and/or numbering-up.
Resources and products		
Feedstock (resource)	The proposed system shall operate with various biomass feedstock, that is, with different composition, in the anaerobic digestion reactor.	The system was assessed for different biomass types including spent grape marc, mustard seed, bagasse, piggery, and poultry with exergy efficiency 0.5–0.6.
Products; intermediate and final	It produces green CH_4 from biomass (black CO_2-neutral) and finally, blue hydrogen, the produced carbon black from the thermal plasma reactor is returned to the agricultural activities.	In the small-scale production of ammonia (0.2 t/day), at 2500°C operating with spent grape marc as a feedstock and biomethane production of ~4.7 kg/h, the proposed system produces ~3.5 kg/h solid carbon, which is directly fed into the agricultural sector for soil conditioning and moisture repair conditioner.
Energy		
Energy source	The proposed system shall operate with renewable energy such as wind and solar PV.	The number of wind turbines required and also the solar PV area required for the system was identified at different geographical locations. Using these real-life data for wind and solar irradiance profile, it was demonstrated that the system can be hybridized with solar PV, wind and storage battery.
Energy integration	Using a steam power block and a waste heat recovery from hydrogen produced by thermal plasma, the system shall generate steam and electricity, which can be used for the nonthermal plasma reactor.	It was identified that a self-sustaining fraction of 0.44 to 0.8 of the total energy requirement of the nonthermal plasma unit can be obtained depending on the temperature of the thermal plasma reactor.

terms of resource, production capacity, and energy efficiency/circularity. We add here a helicopter view mirroring those technological assessments to the challenges of the industrial transformation, as described in the introduction and being accelerated by COVID. This will give a holistic and business-oriented conclusion of the resiliency opportunities. Table 7 summarizes the insight gained on the holistic resilient opportunities provided by the new integrated technology here.

6 | CONCLUSIONS

At the example of ammonia as one of the top-3 globally largest manufactured chemicals, we have explored the feasibility of integrated local, resilient and self-sufficient manufacturing of this major fertilizer product. As a starting point, biomass anaerobic digestion to biogas was taken and ammonia is the end-product (with an option to make nitric acid and nitrates as well). To judge the economic validity, we have performed an exergy assessment for the triple-integrated chemical process from biomass to ammonia; integrating the following real-life industrial directives as an essential part of our theoretical study.

- Peats Soil Company fertilizer manufacture: Point of manufacture at the industrial site: taking data from a commercial product and business opportunity
- South Australian No-Till Farmer Association (SANTFA) advice: personalization of fertilizer product, customized for individual users, with user-friendly enhanced and environmentally benign product functionality
- AgGrow Energy Resources Company (AER) advice: utilization of waste to energy and renewable bioenergy strategies relevant to Australia; and potentially globally.

We developed a process concept leveraging a new production technology to enable:

- quick response and just-in-time production,
- product variety at multiple scales of production,
- resource efficiency and improved environmental sustainability, as they become mature,
- enhanced designer/producer/end-use opportunity.

On this background, we could demonstrate:

- Exergy, thermodynamic feasibility: Thermochemical equilibrium analysis showed that the exergy efficiency of the system strongly depends on the production scale, however, it is always above the threshold of 0.21 (useful exergy efficiency threshold).
- Self-sustaining: part of the energy requirement of the nonthermal reactor can be covered by electricity production using steam produced by heat recovery from thermal plasma plant.
- Local manufacturing capability: the system is flexible to the source of energy and type of feedstock depending on the location of the plant. The process offered the potential to be hybridized with wind and solar energy.
- Self-sufficiency: Ammonia is utilized as fertilizer and generates crops such as grape marc or mustard seed, which create food waste and feed animals to create animal waste (to generate ammonia again using the proposed process).
- Resilience: The proposed system was resilient against engineering, geo-economics, location, feedstock and type of energy resources.
- Local adaptability: the capability (scale of production) of the anaerobic digestion and the nonthermal plasm plants are low, and do not match the upper scale of the thermal plasma plant. Those technological current shortcomings prevent the use on a national and state level. The use at a regional level is potentially possible, yet needs considerable process intensification to be economically viable; besides fulfilling basic requirements of plant size. Yet within those limitations, the proposed system can be tuned with the local needs and end-user requirement, and thereby is not economically dependent on a specific feedstock.
- Environmental friendliness: The solid carbon and also the CO_2 produced in the system is sourced from biomass, hence the process is carbon-neutral and does not contribute to the emission of greenhouse gases. Also, hybridization with renewable energy such as solar and wind can promote economic viability and the final leveled cost of energy.

7 | OUTLOOK

A changing world economy asking for new ways of manufacturing and emerging disruptive technologies converge these days. The research reported in this manuscript tries to open a new chapter in this large stream. The COVID pandemic has accelerated this transformation. The creation of new markets by underwriting a bookbuild is the key. Translational technologies as presented here help to support the reskilling of lateral and intransigent researchers and to build an ecosystem that supports high-value skills, which engages Australia's raw materials and agriculture. The future will mirror how the

presented concept can contribute to improving the resilience of the Australian economy by diversification.

Developing Northern Australia initiatives are at the forefront of many innovative sustainability initiatives and maybe the consummate test case for local, integrated, and circular technologies such as the biomass-to-fertilizer process proposed here. This technology can fill a missing link for those initiatives, and, in turn, be fine-tuned and put on the scales by serving a real-life business case.

In the North West of Western Australia, in the remote Pilbara and Kimberleys there is a specific opportunity to utilize mine dewatering resources to create valuable irrigation food, fiber, fodder and forestry crops.[59] In the last 2 years alone over 80 new irrigation projects have started in these remote country locations. However, fertilizer nutrients and especially nitrogen for grasses and high protein crops have to be trucked in from over 1000 km away. Regionally produced sustainable and preferably organic nutrients that substitute costly imported fertilizers would be a welcome and highly cost-effective alternative. Technical challenges of this proposed process are foreseen yet there are some suggestions to direct future research as follows:

1. Higher energy demand The electric energy required for the nonthermal plasma process to NOx and ammonia is several times larger than for current centralized processes. Thus, there are two essential ways to make that gap smaller, resulting in the commercial applicability of the plasma plants. First, the energy must be taken from a renewable one such as solar or wind energy. Second, heat recovery and power cycle are needed to recycle a portion of the energy back into the system, and we have defined a self-sustaining parameter.
2. Storage capacity In Australia, solar energy is available in most of the locations with reasonable efficiency. Adiurnal and global solar profiles with sufficient exergy can be received from 7 am to 8 pm excluding cloudy sky or shadow effect. Hence 10–12 h of storage capacity via a battery storage system can plausibly provide sufficient energy for driving the process at night. However, such a large capacity of storage will affect the techno-economic viability and final levelized cost of energy (LCOE) of the system. In the present study, a techno-economic view and energy price analysis were not the goals of the present study. However, this is being investigated in another research, which we do currently leveraging the real-life system of a solar farm and its large-scale battery units at our Roseworthy campus, which is an agricultural research ecosystem with cattle and other study foci, outside of Adelaide in the rural area. The goal is to show if our plasma reactors can be run with intermittent energy alone without the need for expensive storage units; meaning with varying degrees of conversion and changes between those within minutes. That promise has always been assigned to plasma process technology, yet the proof is outstanding.
3. LCA emissions of renewables Commensurate with this, the proposed system offers a green approach by minimizing the emission of greenhouse gases by introducing a plasma reactor using renewable resources. Also, carbon dioxide is only formed in the biomass anaerobic digestion reaction, which is a green CO2 and is sourced from biomass. Hence, it does not contribute to global warming. We admit that LCA emissions arise in the full life cycle of renewable energy systems such as concerning the construction, maintenance, and operations of such systems; yet at a level much lower than for fossil fuels. Common databases such as EcoInvent include such small emissions. Even if such emissions would make a difference, a change from a solar to a hydrothermal system could be an option.

ACKNOWLEDGMENTS

The authors acknowledge support from the ERC Grant Surface-COnfined fast modulated Plasma for process and Energy intensification (SCOPE) from the European Commission with the Grant No. 810182. Laurent Fulcheri acknowledges travel support by the University of Adelaide (funding from Pro-Vice Chancellor [International]), which allowed to develop the idea and concept for this research by face-to-face discussions with the Adelaide researchers and South Australian farmers.

AUTHOR CONTRIBUTIONS

Volker Hessel: Conceptualization; investigation; methodology; project administration; resources; supervision; writing-original draft; writing-review & editing. **Mohammad Sarafraz:** Conceptualization; investigation; methodology; software; validation; writing-original draft; writing-review & editing. **Nam Tran:** Conceptualization; formal analysis; project administration; resources; validation; writing-original draft; writing-review & editing. **Hung Nguyen:** Data curation; project administration; resources; validation. **Laurent Fulcheri:** Conceptualization; data curation; methodology; resources; supervision; validation. **Peter Waldewitz:** Conceptualization; data curation; resources. **Rachel Burton:** Data curation; methodology; resources; validation. **Gregory Butler:** Conceptualization; data curation; formal analysis; methodology; resources; validation. **Lawrence Kirton:** Conceptualization; data curation; resources; visualization.

DATA AVAILABILITY STATEMENT

The data that support the findings of this study are available from the corresponding author upon reasonable request.

ORCID

Volker Hessel https://orcid.org/0000-0002-9494-1519

REFERENCES

[1] J. Mokyr, C. Vickers, N. L. Ziebarth, *J. Econ. Perspect.* **2015**, *29* (3), 31.

[2] F. Piccinno, R. Hischier, S. Seeger, C. Som, *J. Cleaner Prod.* **2016**, *135*, 1085.

[3] J. M. Clomburg, A. M. Crumbley, R. Gonzalez, *Science* **2017**, *355*(6320), aag0804.

[4] F. T. Moore, *Q. J. Econ.* **1959**, *73*(2), 232.

[5] D. Ivanov, *Transp Res E* **2020**, *136*, 101922.

[6] M. Nicola, Z. Alsafi, C. Sohrabi, A. Kerwan, A. al-Jabir, C. Iosifidis, M. Agha, R. Agha, *Int J Surg* **2020**, *78*, 185.

[7] Staff, I, COVID-19 is Coming for the Chemical Industry in 2020, BASF Predicts. in *Industrial Week*, Endeavor Business Media, Ohio, USA **2020**.

[8] D. Baqaee, E. Farhi, Nonlinear Production Networks with an Application to the Covid-19 Crisis *Natl Bur Econ Res* **2020**. (27281).

[9] A. Cappelli, E. Cini, *Trends Food Sci. Technol.* **2020**, *99*, 566.

[10] Hegadekatti, K., Post COVID-19 fractal economics and economies. **2020**.

[11] N. N. Taleb, *Antifragile: Things that Gain from Disorder*, Vol. 3, Random House Incorporated, New York City, United States **2012**.

[12] NCCC, Manufacturing Taskforce: Interim report. 2020: Australia.

[13] S. Pookulangara, A. Shephard, *J. Retail. Consum. Serv.* **2013**, *20* (2), 200.

[14] S. Dong, R. J. S. D. Burritt, Cross-sectional benchmarking of social and environmental reporting practice in the australian oil and gas industry. **2010**, *18*(2), 108.

[15] A. Khaliq et al., *Resources* **2014**, *3*(1), 152.

[16] J. Guthrie, S. Cuganesan, L. Ward, Industry specific social and environmental reporting: The Australian Food and Beverage Industry. in *Accounting Forum*, **2008**, *31*(1), p. 1.

[17] Drew, J., M.-A. Young, and M. Tothill, The *Aust J Emerg Manag* **2018**. *33*(4): p. 14.

[18] S. Vitols, *Compet. Chang.* **2002**, *6*(3), 309.

[19] E. Filos, *Int. J. Comput. Integr. Manuf.* **2017**, *30*(1), 15.

[20] Gürsel, I.V., The chemical plant of tomorrow and the future.

[21] V. J. G. P. Hessel, Synthesis, Electrification of chemistry: what is the synergy between plasma synthesis and chemical plant modularization? **2015**, *4*(4), 257.

[22] C. Bramsiepe, G. J. C. I. T. Schembecker, 50% Idea: modularization in process design. **2012**, *84*(5), 581.

[23] Q. H. Pho et al., Perspectives on plasma-assisted synthesis of N-doped nanoparticles as nanopesticides for pest control in crops *React Chem Eng*. **2020**,*5*, p. 1374.

[24] B. Patil et al., Plasma-assisted nitrogen fixation reactions. in *Alternative Energy Sources for Green Chemistry*, Royal Society of Chemistry, Cambridge, UK **2016**, p. 296.

[25] J. J. J. M. T. R. Brightling, *Johnson Matthey Technol Rev* **2018**, *62*(1), 32.

[26] M. Dawud, *Architecture Against Global Warming: A Research Institute for Sustainable Agriculture*, Carleton University, Ontario, Canada **2017**.

[27] D. K. Ojha et al., *ACS Sustain. Chem. Eng.* **2019**, *7*(23), 18785.

[28] E. Cussler et al., *J JoVE* **2017**, *126*, e55691.

[29] M. J. Palys, A. Allman, P. Daoutidis, *Ind. Eng. Chem. Res.* **2018**, *58*(15), 5898.

[30] A. Anastasopoulou et al., *Processes* **2016**, *4*(4), 54.

[31] I. V. Gürsel et al., *Green Process Synth* **2012**, *1*(4), 315.

[32] A. P. Sturman, N. J. Tapper, *The Weather and Climate of Australia and New Zealand*, Oxford University Press, USA **1996**.

[33] E. Nkonya, A. Mirzabaev, J. von Braun, *Economics of Land Degradation and Improvement: A Global Assessment for Sustainable Development*, Springer Nature, Basingstoke, United Kingdom **2016**.

[34] S. S. Kalkhoran et al., *Agric. Syst.* **2019**, *176*, 102684.

[35] Y. Nakagawa, M. Tamura, K. Tomishige, *Fuel Process. Technol.* **2019**, *193*, 404.

[36] J. V. Haveren, E. L. Scott, J. Sanders, *Biofuels Bioprod Biorefin* **2008**, *2*(1), 41.

[37] S. Li et al., *Processes* **2018**, *6*(12), 248.

[38] W. Wang et al., *ChemSusChem* **2017**, *10*(10), 2145.

[39] A. Anastasopoulou et al., *J. Phys. D. Appl. Phys.* **2020**, *53*(23), 234001.

[40] A. Anastasopoulou, S. Butala, J. Lang, V. Hessel, Q. Wang, *Process Design and Environmental Assessment of Plasma-Assisted Nitrogen Fixation Incorporating Renewables*, Czech Society of Chemical Engineering, Prague, Czech Republic **2016**, p. 972.

[41] L. Zhang, Q. Wang, V. Hessel, Green chemistry metrics and life cycle assessment for microflow continuous processing. in *Handbook of Green Chemistry: Online*. Wiley, New Jersey, United States **2010**, p. 157.

[42] M. M. Sarafraz, N. N. Tran, N. Pourali, E. V. Rebrov, V. Hessel, *Energy Convers. Manage.* **2020**, *210*, 112709.

[43] L. Ye et al., *Chem* **2017**, *3*(5), 712.

[44] M. Gautier, V. Rohani, L. Fulcheri, *Int. J. Hydrogen Energy* **2017**, *42*(47), 28140.

[45] D. Li, V. Rohani, F. Fabry, A. Parakkulam Ramaswamy, M. Sennour, L. Fulcheri, *Appl. Catal., B* **2020**, *261*, 118228.

[46] L. Fulcheri, Y. Schwob, *Int. J. Hydrogen Energy* **1995**, *20* (3), 197.

[47] I. Angelidaki, L. Ellegaard, B. K. Ahring, Applications of the anaerobic digestion process. in *Biomethanation II*, Springer, Berlin, Germany **2003**, p. 1.

[48] B. S. Patil et al., Deciphering the synergy between plasma and catalyst support for ammonia synthesis in a packed dielectric barrier discharge reactor *J. Phys. D Appl. Phys.* **2016**, *53*(14), p.144003.

[49] Land Management and Farming in Australia. **2018**: https://www.abs.gov.au/ausstats/abs@.nsf/Lookup/4627.0main%20features82016-17.

[50] Aguilar, J.G., Deme, I, Fulcheri, L., Gruenberger, T.M., Fabry, F., Flamant, G, Ravary, B, 3D modelling of carbon black formation and particle radiation during methane cracking by thermal plasma. *High Temperature Material Processes:*

An International Quarterly of High-Technology Plasma Processes, BEGELL HOUSE Inc., New York, United States **2003**. 7(1).
[51] E. C. Neyts et al., *Chem. Rev.* **2015**, *115*(24), 13408.
[52] E. C. Neyts, A. Bogaerts, *J. Phys. D: Appl. Phys.* **2014**, *47*(22), 224010.
[53] B. Khiari, M. Jeguirim, *Energies* **2018**, *11*(4), 730.
[54] J. Miller, T. J. Foxon, S. Sorrell, *Energies* **2016**, *9*(11), 947.
[55] D. M. Teferra, W. Wubu, Biogas for Clean Energy. in *Anaerobic Digestion*, IntechOpen, London, United Kingdom **2018**.
[56] N.A.W.M.A (NAWMA), *Renewable Energy Park*, South Australia, Nawma **2019**.
[57] B. Igliński, G. Piechota, P. Iwański, M. Skarzatek, G. Pilarski, 15 Years of the Polish agricultural biogas plants: Their history, current status, biogas potential and perspectives *Clean Techn. Environ. Policy* **2020**, *22*(2), p. 281.
[58] A. Anastasopoulou, R. Keijzer, B. Patil, J. Lang, G. Rooij, V. Hessel, *J. Ind. Ecol.* **2020**, *24*, 1171.
[59] DAFWA, *Irrigation in the Pilbara*, The Department of Primary Industries and Regional Development (DPIRD), Western Australia **2016**.

SUPPORTING INFORMATION

Additional supporting information may be found online in the Supporting Information section at the end of this article.

How to cite this article: Sarafraz MM, Tran NN, Nguyen H, et al. Tri-fold process integration leveraging high- and low-temperature plasmas: From biomass to fertilizers with local energy and for local use. *J Adv Manuf Process*. 2021;3:e10081. https://doi.org/10.1002/amp2.10081